International Journal of Nanomedicine

Dovepress
open access to scientific and medical research

Open Access Full Text Article

ORIGINAL RESEARCH

Induction of Robust Immune Responses by CpG-ODN-Loaded Hollow Polymeric Nanoparticles for Antiviral and Vaccine Applications in Chickens

This article was published in the following Dove Press journal:
International Journal of Nanomedicine

Shu-Yi Lin[1]
Bing-Yu Yao[2]
Che-Ming Jack Hu[2,3]
Hui-Wen Chen[1,3]

[1]Department of Veterinary Medicine, National Taiwan University, Taipei, Taiwan; [2]Institute of Biomedical Sciences, Academia Sinica, Taipei, Taiwan; [3]Research Center for Nanotechnology and Infectious Diseases, Taipei, Taiwan

Background: Poultry vaccine has limited choices of adjuvants and is facing severe threat of infectious diseases due to ineffective of widely used commercial vaccines. Thus, development of novel adjuvant that offers safe and effective immunity is of urgent need.

Materials and Methods: The present research engineers a novel chicken adjuvant with potent immune-potentiating capability by incorporating avian toll-like receptor 21 (TLR21) agonist CpG ODN 2007 with a poly(lactic-co-glycolic acid) (PLGA)-based hollow nanoparticle platform (CpG-NP), which subsequently assessed ex vivo and in vivo.

Results: CpG-NPs with an average diameter of 164 nm capable of sustained release of CpG for up to 96 hours were successfully prepared. With the ex vivo model of chicken bone marrow-derived dendritic cells (chBMDCs), CpG-NP was engulfed effectively and found to induce DC maturation, promoting dendrite formation and upregulation of CD40, CD80 and CCR7. In addition to enhanced expression of IL-1β, IL-6, IL-12 and IFN-γ, 53/84 immune-related genes were found to be stimulated in CpG-NP-treated chBMDCs, whereas only 39 of such genes were stimulated in free CpG-treated cells. These upregulated genes suggest immune skewing toward T helper cell 1 bias and evidence of improved mucosal immunity upon vaccination with the CpG-NP. The CpG-NP-treated chBMDCs showed protective effects to DF-1 cells against avian influenza virus H6N1 infection. Upon subsequent coupling with infectious bronchitis virus subunit antigen administration, chickens were immunostimulated to acquire higher humoral immune response and protective response against viral challenge.

Conclusion: This work presents a novel hollow CpG-NP formulation, demonstrating effective and long-lasting immunostimulatory ability ex vivo and in vivo for chickens, as systemically compared to free CpG. This enhanced immune stimulation benefits from high stability and controlled release of internal component of nanoparticles that improve cellular delivery, lymphoid organ targeting and sustainable DC activation. CpG-NP has broad application potential in antiviral and vaccine development.

Keywords: polymeric hollow nanoparticle, CpG, adjuvant, antiviral response, influenza virus, infectious bronchitis virus, vaccine

Introduction

Poultry industry provides a large amount of affordable meat and eggs, sustaining people's need for animal protein and nutrition. However, poultries are facing great threats from many respiratory infectious diseases, including avian influenza, Newcastle disease and infectious bronchitis. In practical applications, vaccination to the susceptible herds is a common method to protect poultry from pathogen

Correspondence: Hui-Wen Chen
Department of Veterinary Medicine, National Taiwan University, 1 Sec 4 Roosevelt Road, Taipei 10617, Taiwan
Tel +886 2 33669450
Email winnichen@ntu.edu.tw

submit your manuscript | www.dovepress.com
DovePress
http://doi.org/10.2147/IJN.S241492

© 2020 Lin et al. This work is published and licensed by Dove Medical Press Limited. The full terms of this license are available at https://www.dovepress.com/terms.php and incorporate the Creative Commons Attribution – Non Commercial (unported, v3.0) License (http://creativecommons.org/licenses/by-nc/3.0/). By accessing the work you hereby accept the Terms. Non-commercial uses of the work are permitted without any further permission from Dove Medical Press Limited, provided the work is properly attributed. For permission for commercial use of this work, please see paragraphs 4.2 and 5 of our Terms (https://www.dovepress.com/terms.php).

infection. While conventional vaccines are widely used, various disadvantages, such as virulence reversion of live attenuated vaccine and incomplete immune response of inactivated vaccine, present major logistical and practical concerns. With these lingering concerns associated with traditional vaccines, there is continuing interest in the development of novel subunit protein, DNA vector and virus-like particle vaccines. Among efforts to promote poultry health, strategies to enhance innate immune activation for direct antiviral treatment as well as for improving adaptive immune responses to vaccines are of major scientific and agricultural interest.

The use of adjuvants in vaccination has offered many advantages, including dose sparing, immunization number reduction, faster initial responses, potent specific anti-pathogen responses and longer lasting immune memory. Traditional adjuvants, such as the aluminum salt, enhance antigen immunogenicity via a depot mechanism by converting soluble antigen to a particulate form. Despite significant enhancement of serum humoral response upon supplementing vaccine with the aluminum adjuvant,[1] induction of cell-mediated immune response remains poor.[2] Aside from aluminum salts, emulsified complete Freund's adjuvant and incomplete Freund's adjuvant frequently associated with animal vaccination[3] However, their side effect in inducing abscesses and granuloma at the injection site could affect the quality of chicken meat. Moreover, with the increasing attention to food safety, non-toxic and biodegradable adjuvants for chickens would be favored to prevent the accumulation effect of potential toxic substances from food to humans. These factors incentivize advancement of safe, potent adjuvants in avian vaccine development.

Towards innate immune activation, toll-like receptor (TLR) activation by molecular agonists such as lipoproteins, flagellin, and oligonucleotides has been frequently explored. Among them, oligonucleotides rich in CpG motifs, a feature commonly found in bacterial DNA, presents a potent danger signal.[4] In mammals, TLR9 recognizes CpG motifs and thereafter mediates the induction of cell signaling pathways,[5] and TLR21 is a functional counterpart of TLR9 in chickens and other poultry animals.[6] Synthetic oligodeoxynucleotides (ODN) containing CpG motifs have been shown to activate host immune responses and act as immunostimulants in chickens, leading to immune protection against *Escherichia coli* and *Salmonella typhimurium*.[7,8] CpG ODN has also been used as an adjuvant in chicken antiviral studies and can be administrated orally, intranasally, subcutaneously and in ovo.[9–11] Class B CpG ODN, in particular CpG ODN 2007, can stimulate strong B cell and NK cell responses and NF-κB signaling pathway.[12,13] The adjuvant has been shown to induce significant enhancement of antibody, cytokines and splenocyte proliferation in vaccine formulations to defend against avian influenza virus (AIV), infectious bronchitis virus (IBV) and Newcastle disease virus.[9–11,14] Thus, CpG ODN 2007 serves as a compelling adjuvant with the potential to induce potent humoral and cellular immunity for avian infectious diseases vaccination.

CpG is a molecular adjuvant that can diffuse and degrade rapidly upon entering physiological environment. As such, the use of nanocarriers for adjuvant delivery offers many advantages as these nanoscale vehicles can protect the fragile adjuvant cargo during their transport. Nanoparticles can be more effectively accumulated to lymphoid tissues either through engulfment and transportation mediated by migratory dendritic cells or through free, diffusive movement in lymphatic vessels. Also, owing to the synthetic flexibility of nanomaterials, particle size, shape, surface properties, and adjuvant contents can be elaborately designed to tailor to specific innate immune induction and targeting to specific immune cells. Through nanoparticle encapsulation or surface conjugation, TLR agonists including CpG and poly (I:C) have been tested to enhance immunostimulatory ability on mice model.[15–17] Among various nanomaterials, poly(lactic-co-glycolic acid) (PLGA) is one of the most commonly used polymer for delivery applications owing to its biocompatibility and biodegradability. Various forms of PLGA nanoparticles have been prepared to combat pressing human infections, including influenza, dengue, malaria, and Middle East respiratory syndrome coronavirus.[18,19] For applications in chickens, CpG-loaded PLGA particles have been applied in combination with inactivated influenza vaccine.[20] However, the large particle diameter (682.03 nm) for the particulate adjuvant in the study may have hammered its transport to the lymphoid tissues,[20] resulting marginal improvement in vaccine effectiveness. There is also a lack of mechanistic evaluation assessing the molecular basis of nanoparticle-mediated adjuvant enhancement. Towards combatting avian infections, the present research adopts a recently developed PLGA-based hollow nanoparticle for CpG delivery.[18] The adjuvant uptake, dendritic cell activation, immunity-related gene expression, and antiviral ability were rigorously assessed and compared between free CpG and CpG-NP. Also, in vivo immunostimulating efficacy as a vaccine adjuvant was evaluated upon coupling with a subunit protein antigen. This study highlights a flexible hollow nanoparticle platform that is able to tailor contents for

various demands, demonstrating broad application in antiviral and vaccine development.

Materials and Methods

Cells, Viruses, Animals

Chicken embryo fibroblast cell DF-1 and Madin-Darby Canine Kidney cells (MDCK) were purchased from American Type Culture Collection (ATCC) and maintained at 37°C in DMEM medium supplemented with 10% FBS and 1% antibiotic-antimycotic. *Spodoptera frugiperda* Sf9 and Sf21 cells were purchased from Invitrogen (Carlsbad, CA). Sf9 cells were cultured at 27°C in Grace's insect cell medium supplemented with 10% FBS and 1% antibiotic-antimycotic. Serum-free adapted Sf21 cells were cultured in Sf-900 II containing 0.25% antibiotic-antimycotic. All the cell culture medium and reagents were purchased from Gibco. AIV strain A/Duck/Yilan/2904/99(H6N1)[21] was propagated in specific pathogen-free (SPF) embryonic eggs (JD-SPF Biotech, Miaoli, Taiwan) and the viral titer ($TCID_{50}$) was titrated in MDCK cells. The plaque-forming unit was assumed as 0.7 x $TCID_{50}$ according to the Poisson distribution. IBV strain 2296/95 was propagated and titrated (EID_{50}) in SPF embryonic eggs.[22,23] For animal experiments, SPF chickens (JD-SPF Biotech) were housed in the animal facility at the National Taiwan University. All animal experiments were performed under an approved Institutional Animal Care and Use Committee (IACUC) protocol (no. NTU-105-EL-00174).

Preparation of Chicken Bone Marrow-Derived Dendritic Cells

Chicken bone marrow-derived dendritic cells (chBMDCs) were prepared as previously described[24] for the test. Briefly, the 2–4 wk-old SPF chicken were sacrificed for bone marrow cells from femurs. Total cells were flushed with cold sterile PBS and passed through 70 μm cell strainer (Falcon). After PBS wash and resuspension, cells were isolated in same volume of Histopaque-1119 (Sigma-Aldrich) under density gradient centrifugation 1000×g, 30 min. The interphase was collected and washed twice with cold sterile PBS. Cells were then cultured in RPMI-1640 medium containing 10% chicken serum, 1% antibiotic-antimycotic and 1% non-essential amino acid (all from Gibco) in the presence of 10 ng/mL recombinant chicken interleukin-4 (IL-4) and granulocyte-macrophage colony-stimulating factor (GM-CSF) (both from Kingfisher Biotech, Saint Paul, MN) for 6 days for DC differentiation.

Preparation of CpG-Loaded Nanoparticles

The immunostimulatory CpG ODN 2007 (5′-tcgtcgttgtcgttttgtcgtt-3′) was purchased from Invivogen (San Diego, CA). Using a water in oil in water (w/o/w) double emulsion technique, CpG-encapsulating PLGA thin-shell nanoparticles (CpG-NP) were prepared as described previously.[18] Briefly, a polymer solution was prepared by dissolving 50 mg of PLGA (poly(dl-lactide-co-glycolide, purchased from LACTEL Absorbable Polymers)) in dichloromethane. The inner aqueous phase was prepared by dissolving CpG in the phosphate buffer (pH 7). For a typical preparation, 50 μL of aqueous solution containing 125 μg of CpG was emulsified in 500 μL of polymer solution in ice using an ultrasonic probe sonicator under the pulse mode with 40% amplitude and on-off durations of 1 and 2 s for 1 min. The first emulsion was subsequently added to 5 mL of 10 mM phosphate buffer (pH 7), which was then probe sonicated at 30% amplitude with on-off durations of 1 and 2 s for 2 min. The emulsion was subsequently poured to 8 mL of water and heated at 40°C under gentle stirring in a fume hood for solvent evaporation. Following solvent evaporation for 1 hr, the nanoparticles were collected by 30,000 ×g centrifugation and resuspended in 10% sucrose solution. The CpG content was analyzed by the reagent in Quant-iT™ RiboGreen® RNA Kit (Invitrogen). For preparing fluorescently labelled nanoparticles (CpG-Cy5-NP), 15 μg of Sulfo-Cyanine5 (Cy5) fluorescent dye (Lumiprobe, Hunt Valley, MD) was additionally added to the solvent phase during the emulsion process. Empty hollow nanoparticles without CpG loading were also prepared as control particles. For the stability test, CpG-NPs were stored at −20°C for 1 month or placed at 4°C or 24°C (room temperature) for 7 days. The CpG content and the size of nanoparticles were determined and compared before and after storage and at predetermined time points.

Transmission Electron Microscopy (TEM) and Dynamic Light Scattering (DLS)

Nanoparticles were characterized for the physicochemical properties through a combination of analytical techniques including dynamic light scattering (DLS), transmission electron microscope (TEM) and cryo-EM. Nanoparticle size and surface charge were measured by DLS with Malvern Zetasizer Nano ZS (Malvern Instrument) according to the manufacturer's instructions. Negative staining was applied for TEM observation. First, 10 μL nanoparticles was loaded onto a glow-discharged grid, and the droplet was remained on the grip for 10 sec and subsequently removed by a filter paper. Excessive nanoparticles

were washed out by ddH_2O loaded to the grid. Then, 1% uranyl acetate was applied to the grid for 30 sec for negative staining. Next, prepared grids were air dried and stored at 40–50% humidity until TEM observation using an FEI 120 kV Sphera microscope. Cryo-EM images were acquired using a Tecnai F20 transmission electron microscope operating at an acceleration voltage of 200 kV.

Release Kinetics of CpG Nanoparticles

The release kinetics was determined in 10 mM sodium phosphate buffer (pH 7.0) and 10 mM acetate buffer (pH 5.0). The Slide-A-Lyzer MINI Dialysis units (10 kDa MWCO, Thermo Fisher Scientific) were loaded with 100 μL of CpG-encapsulated nanoparticles and placed in tanks containing aforementioned buffers at 37°C. After 15 min, 30 min, 1, 2, 4, 8, 24, 48, 72 and 96 hr, the nanoparticles remaining in dialysis units were collected and disrupted by 100% acetone. After acetone was evaporated, remaining CpG was analyzed by the reagent in Quant-iT™ RiboGreen® RNA Kit (Invitrogen).

Cellular Uptake of CpG Nanoparticles

The cellular uptake of nanoparticles by immature chBMDC was studied by treating cells with 200 ng/mL of CpG and Cy5 dye co-encapsulated nanoparticles (CpG-Cy5-NP). After 3, 8 and 16 hr treatment, intracellular fluorescence images were recorded by Olympus IX-83. By 48 hr after treatment, cells were fixed with the cold acetone for 10 min, and cellular nuclei were stained with DAPI. Fluorescence images were acquired by Olympus IX-83.

Safety Test in vitro

The safety of different formulation of CpG was assessed via in vitro cytotoxicity study. Immature chBMDCs were incubated with various (2, 20, 200 ng/mL) concentrations of the free (unencapsulated) CpG or CpG-NP for 72 hr, and the cellular viability was evaluated using an alamarBlue Cell Viability Reagent (Thermo Fisher Scientific). Untreated cells were used as control.

Evaluation of chBMDC Maturation

The prepared immature chBMDCs were treated by free CpG or CpG-NP for 24 hr. Morphological changes of cells were observed and images were captured under an inverted microscope at 10× magnification. Morphological changes demonstrating DC maturation were analyzed from 9 random microscope fields for each treatment with ImageJ (Version 1.49). In addition, treated chBMDCs were analyzed by FACSCalibur Flow Cytometry (BD Biosciences).

Free CpG or CpG-NP were diluted to 200 ng/mL in the culture medium and added to immature chBMDC cells. Treated chBMDC cultures were harvested 16 hr following incubation and assayed for CD40, CD80 and CCR7 mRNA expression by real-time RT-PCR using primer pairs listed in Table 1. Briefly, total RNA of chBMDC was extracted by Total RNA Mini Kit (Geneaid, Taipei, Taiwan), reverse transcribed by QuantiNova Rev. Transcription Kit (Qiagen) and PCR-amplified by QuantiNova SYBR Green PCR Kit (Qiagen) with Biorad CFX connect real-time system. The PCR procedure is as follows: 95°C 2 min for pre-denaturation, 40 cycles of 95°

Table 1 Primer Pairs for Real-Time RT-PCR

Gene	Sequence (5′–3′)	GenBank Accession No	Ref.
CD40	GGCACCTTCTCCAATGTATCTTC GTTCGTCCCTTTCACCTTCAC	NM204665	[46]
CD80	CAGCAAGCCGAACATAGAAAGA AGCAAACTGGTGGACCTGAGA	NM001079739	[46]
CCR7	CATGGACGGCGGTAAACAG TCATAGTCGTCGGTGACGTTGT	HQ269806	[35]
IL-1β	ACATGTCGTGTGTGATGAG CAGCCGGTAGAAGATGAAGC	NM_204524	[47]
IL-6	GCGAGAACAGCATGGAGATG GTAGGTCTGAAAGGCGAACAG	NM_204628	[47]
IL-12α (p35)	TGGCCGCTGCAAACG ACCTCTTCAAGGGTGCACTCA	AY262751	[24]
IFN-γ	AAGTCAAAGCCGCACATCAAAC CTGGATTCTCAAGTCGTTCATCG	X99774	[48]

Abbreviations: IL, interleukin; CD, cluster of differentiation; CCR, C-C chemokine receptor.

C 5 sec and 60°C 10 sec for segment amplification, and a ramp from 65°C to 95°C for the melting curve analysis.

Immune Gene Activation of chBMDCs

Free CpG and CpG-NP were serially diluted in culture medium and added to chBMDCs. Treated cells were harvested at 2, 4, 8, 16 hr following incubation and assayed for proinflammatory cytokines mRNA expression, including IL-1β, IL-6, IL-12 and IFN-γ, by real-time RT-PCR as described above. Also, a RT^2 Profiler Chicken Innate & Adaptive Immune Responses PCR Array (PAGG-052ZG, Qiagen) was used to measure 84 immune gene activation following 16 hr incubation with 200 ng/mL of CpG. This 384-well PCR array assay used Roche LightCycler 480 (Roche). The PCR array analysis was carried out by online RT2 Profiler PCR Data Analysis System (https://dataanalysis2.qiagen.com/pcr). The C_T value of 40 was set to be the cut-off value, and the β-actin, hydroxymethylbilane synthase and ribosomal protein L4 genes were selected for normalization with their geometric means.

IFN-γ Detection by ELISA

ChBMDCs were mock treated or treated with 200 ng/mL free CpG or CpG-NP for 24 hr, and the culture supernatant was collected and stored at −80°C until use. The presence of IFN-γ in the culture supernatant was detected using the IFN-gamma Chicken Matched Antibody Pair (Invitrogen) according to the manufacturer's instructions. Briefly, the coating antibody was coated onto a 96-well plate (0.2 μg/well) overnight at 4°C. The plate was then blocked with PBS containing 0.5% BSA and 0.1% Tween 20. Next, 100 μL of sample was dispensed into two duplicated wells, followed by adding 50 μL of 1 μg/mL detection antibody. The plate was sealed and incubated at room temperature for 2 hr on a shaker (700 rpm). Following washes with PBS containing 0.1% Tween 20, 100 μL of streptavidin-HRP (1:1024) was added and incubated at room temperature for 30 min on a shaker (700 rpm). Finally, 100 μL of TMB substrate (KPL, Gaithersburg, MD) was applied to each well and incubated at room temperature for 30 min on a shaker (700 rpm) until 1 M H_2SO_4 was added to stop the reaction. A microplate reader (Synergy H1, BioTek, Winooski, VT) was used to read the optical density at 450 nm.

Protective Antiviral Response Induced by CpG Stimulation

Antiviral activity of the chBMDC culture supernatant in response to CpG stimulation was investigated on DF-1 cells. Immature chBMDCs were treated with 200 ng/mL free CpG or CpG-NP for 24 hr, and the culture supernatant was collected and applied onto DF-1 cells for 8 hr incubation. After PBS washes, AIV strain (A/Duck/Yilan/2904/99(H6N1)) was used to infect the DF-1 cells for 2 hr at an MOI of 1 in the infection medium (high glucose DMEM containing 0.075% BSA, 1% NEAA, 1% sodium pyruvate, 1% HEPES, 1% antibiotic-antimycotic, and supplemented with 0.3 μg/mL TPCK-treated trypsin). Next, the virus was removed and replaced with fresh infection medium. After 8 hr incubation, DF-1 cells were collected for the Western blot assay, using mouse anti-influenza nucleoprotein monoclonal antibody (Clone InA108, HyTest) and mouse anti-α-tubulin monoclonal antibody (Clone B-5-1-2, Sigma-Aldrich), both at 1:2000 dilution. Results were developed by Clarity™ Western ECL Substrate (Biorad) and visualized with the ChemiDoc XRS+ imaging system (Biorad). The protein expression levels were analyzed by Image Lab software (Version 5.2.1). In addition, the DF-1 culture supernatants were harvested for viral genome quantification and $TCID_{50}$ assay as previously described.[25,26]

Expression and Purification of IBV Receptor Binding Domain (RBD) Protein

Viral RNA from the allantoic fluid was extracted using the viral nucleic acid extraction kit (Geneaid Biotech Ltd., Taipei, Taiwan) following the manufacturer's protocol. According to the previous study,[27] the fragment that encodes the RBD of spike protein was amplified using one-step RT-PCR with a forward primer carrying the NdeI restriction site (5′-GCCA CATATGACTTTGTATGATAATG-3′) and a reverse primer carrying NotI digestion site and His tag sequence (5′-GACA GCGGCCGCCTAATGATGATGATGATGTTGCTTA-ACTAAGC-3′) (synthesized by Tri-I Biotech, Taipei, Taiwan). The PCR product was subcloned into the yT&A vector (Yeastern Biotech, Taipei, Taiwan). After enzyme (NEB) digestion, the restriction fragment was column-purified and ligated to the pFastBac1-gp67-His-IRES-EGFP vector.[28] The resultant recombinant plasmid was transformed and amplified in *E. coli* DH5a, and further transposed into *E. coli* DH10Bac (Invitrogen) for gene transposition. The transposed bacmid was then purified for transfection and preparation of recombinant baculovirus carrying the gene of interest in Sf9 cells. After two viral passages, Sf21 cells were infected with the recombinant baculovirus at an MOI of 0.01 and incubated for 4 days. The culture supernatant was collected by centrifugation, and the rRBD protein was purified by the HisTrap FF column (GE Healthcare) using GE ÄKTA protein purification system. The purified protein was verified by the SDS-PAGE and Western

blot using IBV spike specific monoclonal antibody (clone 2296-4).[29] Protein concentration was determined by the BCA assay (Pierce).

Chicken Immunization Experiments

Eighteen SPF chickens (JD-SPF Biotech Co., Ltd) were randomly divided into three groups and subcutaneously immunized with PBS, rRBD mixed with free CpG or rRBD mixed with CpG-NP. The chickens were primed at 2-week-old and boosted twice at 5-week-old and 9-week-old. The inoculating dose was 4 μg of CpG (free or encapsulated) and 26 μg of rRBD per chicken. Two weeks after the first boost, chicken sera were collected and anti-rRBD antibody titers were determined by ELISA. Two weeks after the second boost, five chickens per group were challenged with 10^6 EID_{50} of IBV 2296/95. Lung and kidney were collected at 6 days post-challenge and homogenized for virus re-isolation in SPF embryonic eggs.

Antibody ELISA

Hundred nanograms per well rRBD was coated onto the 96-well flat bottom plate (Nunc, Denmark) with the coating buffer (15 mM Na_2CO_3 and 35 mM $NaHCO_3$, pH 9.6). . The plate was washed three times with PBST and blocked with 5% skim milk (BD) for 1 hr. Serially diluted serum was added into the plate (100 μL/well) and incubated for 1 hr. After PBST washes, the rabbit anti-chicken IgY HRP conjugate (Jackson ImmunoResearch) at 1:2000 dilution was added into the plate (100 μL/well) and incubated for another hour. After further PBST washes, TMB substrate (KPL) was applied to the plate (100 μL/well) and incubated in the dark for 10 min until 1 M H_2SO_4 was added to stop the reaction. All the antibody incubation steps were conducted at room temperature. A microplate reader (Synergy H1, BioTek) was used to read the optical density at 450 nm.

Virus Re-Isolation

Chicken lung and kidney were collected in 3 mL of sterile PBS at 6 days post-challenge and homogenized. The homogenates were clarified under 3000×g 10 min centrifugation and stored at −80°C freezer. Each sample was tested in two 9-day-old SPF embryos (JD-SPF Biotech Co., Ltd) and incubated at 37°C for 7 days. Upon examination, demonstration of embryo death, dwarfing and curling indicated the positive results for IBV re-isolation. Sample was determined as positive in virus re-isolation if any of the embryos showed infection.

Statistical Analyses

Data were analyzed by unpaired *t*-tests, one-way ANOVA followed by Tukey's multiple comparison tests or two-way ANOVA followed by Sidak's multiple comparison tests using GraphPad Prism (GraphPad Software, San Diego, CA). The p values smaller than 0.05 were considered statistically significant.

Results

Characterization of CpG-Loaded Polymeric Hollow Nanoparticles

Preparation of thin-shell CpG-loaded PLGA nanoparticle (CpG-NP), as illustrated in Figure 1A, was optimized using a water-in-oil-in-water (w/o/w) double emulsion technique. DLS and TEM imaging were used to characterize the nanoparticles. The results showed that unimodal round shape and thin-shell hollow nanoparticles with an average diameter of 164 nm were observed, and the hollow nanoparticle without the CpG loading was similar in size with the internally loaded nanoparticle. (Figure 1B–D). The zeta-potential was determined as −60.2 mV. The encapsulation efficiency was consistent at approximately 50% when tested with different CpG input (data not shown). The nanoparticle size and CpG encapsulation before and after storage by freezing at −20°C for 1 month were determined. The results showed that the nanoparticles retain the same size and CpG encapsulation following the storage period (Figure 1E and F). In addition, as shown in Figure 1G, the nanoparticle stably retains its CpG cargo at 4°C during the observation period (7 days). At room temperature, however, a loss of ~10% of CpG was observed and attributable to hydrolysis of the polymeric shell. The test of CpG release kinetics of CpG-NPs indicated that PLGA-based CpG-NP was more stable in pH 7.0 than in pH 5.0 (Figure 1H), suggesting the prevention of early disruption of CpG-NPs and loss of adjuvant in general physiological environment. Moreover, the sensitivity to low pH environment facilitates the CpG-NP unloading in acidic endosomes once uptake by cells.

Efficient Intracellular Delivery of CpG to Chicken Immune Cells

In this study, chicken bone marrow-derived dendritic cells were obtained by isolating the bone marrow cells and differentiate into dendritic cells in the presence of chicken IL-4 and chicken GM-CSF. The morphology of chBMDCs was observed under the inverted light microscope. During the 6-day differentiation, the cells became larger with the appearance of several small and bright granules in the

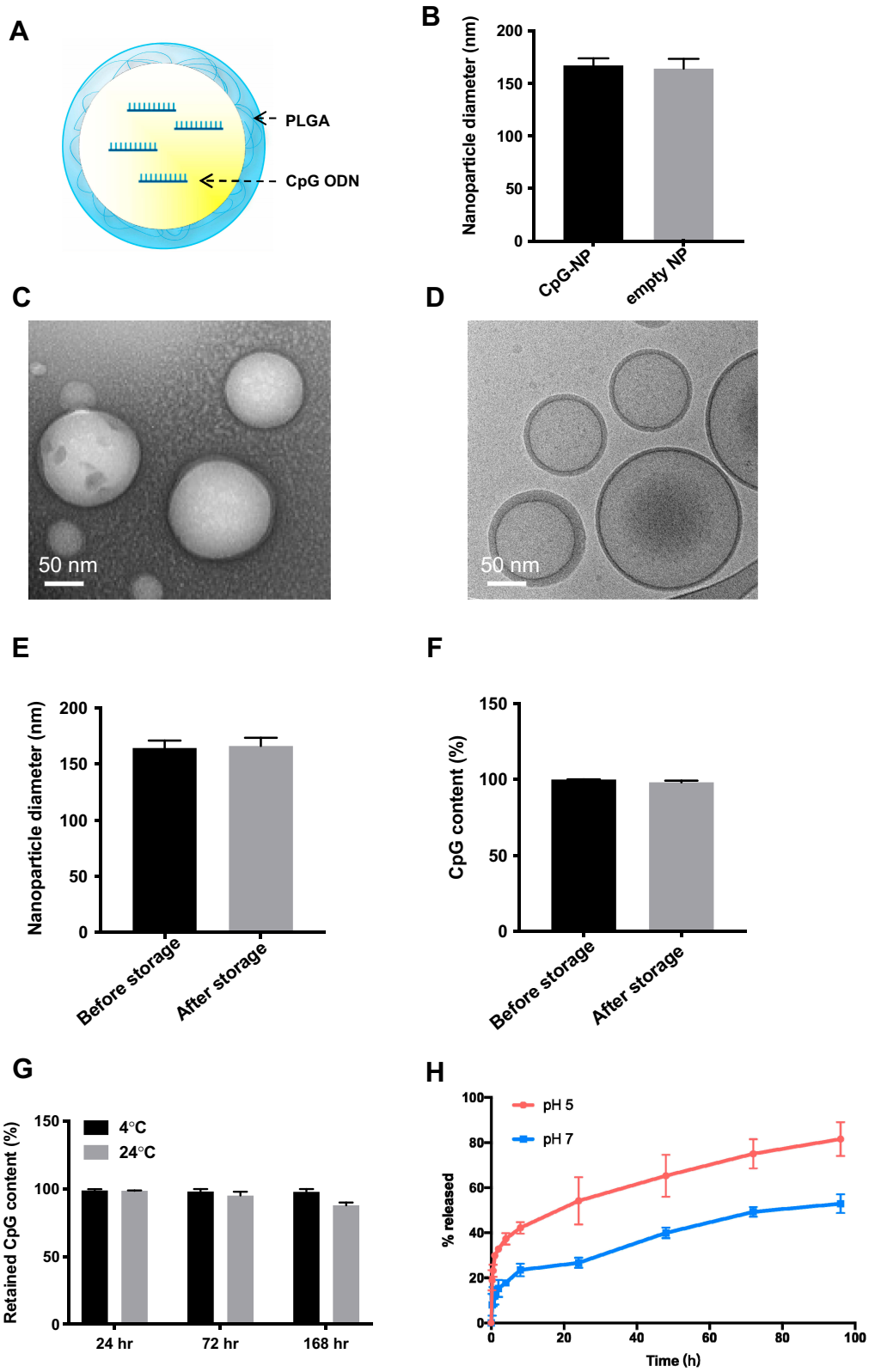

Figure 1 (**A**) Schematic illustration of a PLGA hollow nanoparticle encapsulating CpG (CpG-NP). (**B**) The size of CpG-NP and empty NP as determined by DLS. (**C**) CpG-NPs were visualized using transmission electronic microscopy under negative staining with uranyl acetate. (**D**) Cryo-EM visualization of the CpG-NP reveals its hollow, core-shell structure. (**E**) Nanoparticle size measurement following storage by freezing at −20°C for 1 month. (**F**) CpG content ratio following storage by freezing at −20°C for 1 month. (**G**) CpG content ratio following storage at 4°C or 24°C for 7 days. (**H**) In vitro release kinetic of CpG from CpG-NP at pH 5 and pH 7. Error bars represent mean ± SD, n=3.

cytoplasm (Figure 2A). The larger cytoplasm is one of the characteristics of immature DCs, so-called veiled cells, and the granules, termed intracytoplasmic circular granules, are a phenotypic feature of monocyte-derived dendritic cells.[30,31] However, these cells did not appear to aggregate as previously reported by Wu et al.[24] In contrast to the IL-4 and GM-CSF supplemented cells, the supplemented bone marrow cells remained in an undifferentiated morphology and did not expand in terms of cell numbers during the 6-day culture (Figure 2A).

To confirm the ability of chBMDC to engulf nanoparticles, a CpG and Cy5 fluorescence dye co-encapsulated nanoparticle (CpG-Cy5-NP) was prepared. Following the CpG-Cy5-NP treatment, cellular uptake of nanoparticles was confirmed by the detection of Cy5 in the cytoplasm. The uptake kinetics was observed at 3, 8, 16 (Figure 2B) and 48 hours (Figure 2C). It was found that as early as 3 hr post-treatment, Cy5 signal can be detected in chBMDCs. This signal continuously increased over time until 48 hr post-treatment, and most of the DCs showed abundant fluorescent signal, indicating the nanoparticle-based CpG can be efficiently delivered into immune cells for toll-receptor signaling and innate immunity activation.

ChBMDC Maturation Induced by Nanoparticulated CpG

The alamarBlue assay validated the safety of free CpG or CpG-NPs in chBMDCs as high cell viability was obtained in all tested concentrations of CpG over 72 hr of treatment

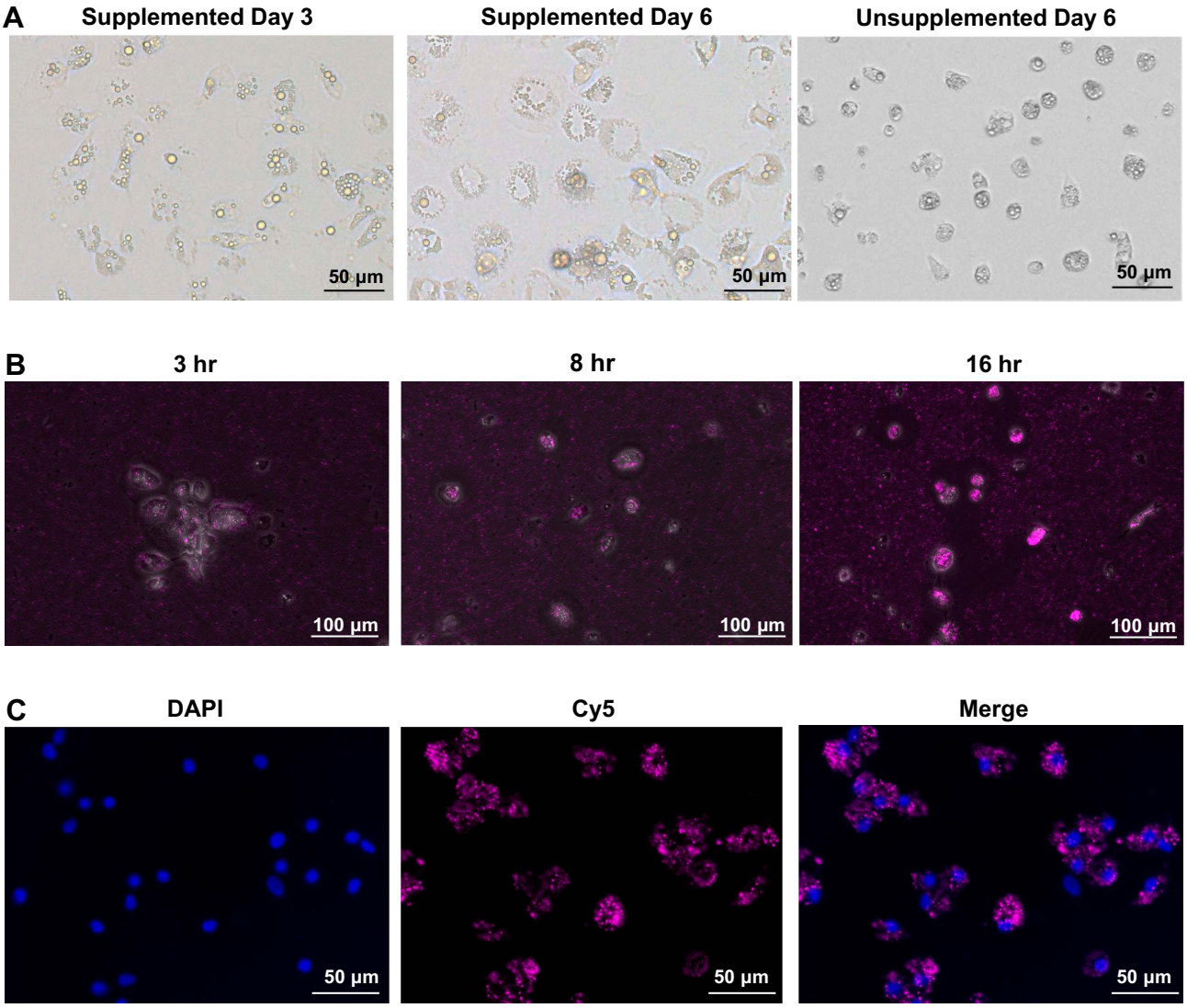

Figure 2 (**A**) Chicken BMDCs supplemented (day 3 and day 6) and unsupplemented (day 6) with recombinant chicken GM-CSF and IL-4. (**B**) Chicken BMDCs were incubated with CpG-Cy5-NP to observe the uptake kinetic at 3, 8, 16 hr post-incubation. (**C**) 48 hr post-incubation, cytoplasmic Cy5 signal was shown with the nucleus stain of DAPI, indicating nanoparticle uptake by chicken BMDCs.

(Figure 3A). ChBMDCs' maturation was assessed by cell morphology and phenotype characterization. After 200 ng/mL of free CpG or CpG-NP treatment for 16 hours, the veiled, granular immature chBMDCs developed dendrites, which is a distinct morphology of mature DC (Figure 3B, arrowed). Comparing with the free CpG-treated group, CpG-NP-treated group showed significantly higher percentage of DC-like cells in the culture (Figure 3C). The CpG-NP-treated cells also displayed distinct intracellular complexity with greater side scatter intensity, indicating that CpG-NP treatment to cells contributed to high granularity of DCs, as analyzed by flow cytometry (Figure 3D). Due to the lack of antibodies for chicken DC surface markers, an alternative method, quantitative PCR, was applied to determine the expression levels of CD40 and CD80, where are two co-stimulators for naïve T cell activation and CCR7, a maturation marker for DCs (Figure 3E). The results show that, comparing to the free CpG-treated group, CpG-NP-treated DCs exhibited greater expression levels of CD40, CD80 and CCR7, suggesting more complete BMDC maturation induced by nanoparticulate CpG.

Enhanced Immune Activation in chBMDCs by Nanoparticulated CpG

To better understand the immune gene profile of chBMDCs in response to free CpG or CpG-NP, a panel of chicken innate and adaptive immune response genes were evaluated by a quantification PCR-based array (Table S1). The BMDCs were incubated for 16 hr with 200 ng/mL of free CpG, CpG-NP or the control empty NP. As shown in Figures 4A and S1, 53/84 immune-related genes (indicated by *) were found to be stimulated (>3-fold increase) in CpG-NP-treated chBMDCs whereas only 39 of such genes were stimulated in free CpG-treated cells, suggesting an enhanced activation in the immune system trigger by the CpG-NP. Treatment of cells with the empty NP exhibited a negligible activation in the immune response. Upon categorization of these immune genes, it was found that TLR signaling genes, such as MyD88 and TRIF (TICAM1) were not upregulated, while the TLR effector genes were upregulated by both of CpG-NP and free CpG. In particular, the expression levels of innate immunity genes, including TLR3, TLR15, NF-κB, IRF7 and several interleukin family genes, were significantly higher in the CpG-NP treated group than the free CpG group (Figures 4B and S1). To further evaluate the dosing effect of CpG treatment, serially diluted CpG in two different formulations was added to chBMDCs and incubated for 16 hr. The gene expression levels of IL-1β, IL-6, IL-12 and IFN-γ in chBMDCs were analyzed by real-time RT-PCR. The results showed that these genes were significantly stimulated by CpG-NP at 200 ng/mL, even at a lower concentration of 20 ng/mL, CpG-NP treatment still induced comparable or greater levels of cytokine genes expression than the highest dose of free CpG (Figure 4D). Furthermore, to evaluate the time course effect, various time points between 2 and 16 hr following incubation with constant 200 ng/mL CpG with two different formulations were analyzed. As indicated in Figure 4E, CpG-NP triggered 3-fold enhancement of IL-1β and IL-6 mRNA expression at 2 hr post-incubation, and the stimulation lasted through 16 hr. For IL-12 and IFN-γ, free CpG-treated group reached an intrinsic peak of gene expression at the 4 hr mark, whereas CpG-NP continuously stimulated gene expression during the 16 hr incubation. A significantly higher production of IFN-γ in chBMDCs in response to CpG-NP stimulation was also confirmed by a sandwich ELISA detection in chBMDC culture supernatant (Figure 4C), and the results are consistent with the findings from the mRNA expression levels. Collectively, as compared to free CpG, CpG-NP showed evidence of more effective and long-lasting immune activation in chBMDCs.

CpG-NP-Primed BMDCs Produced Effective Antiviral Proteins

Since several immune genes were observed to be stimulated by CpG-NP treatment in chBMDC, we sought to know if this activation can contribute to antiviral immunity. Based on the assay procedure illustrated in Figure 5A, the antiviral response elicited by the CpG-NP was examined in the BMDC culture supernatant-pretreated and subsequently AIV-infected DF-1 cells. The results showed that, 8 hr after virus infection, the expression ratio of viral nucleoprotein to the housekeeping gene α-tubulin in CpG-NP-treated group (0.37) was decreased by approximately two-fold, as compared to the mock (untreated) control group (0.66) or free CpG-treated group (0.63) (Figure 5B), indicating the nanoparticulate CpG-primed chBMDCs produced more effective functional components to inhibit virus protein expression. In addition, extracellularly released virus from infected DF-1 cells was examined. CpG-NP group exhibited more than ten-fold reduction on the viral genome copies detected in the culture supernatant, as compared to the free CpG group or mock control group (Figure 5C). Similarly, the virus titer detected from the CpG-NP group was 2-$\log_{10}$ lower than the mock group and significantly lower than the free CpG group (Figure 5D). These results collectively indicate that, comparing with the free CpG formulation, CpG-NP is capable of inducing enhanced antiviral response in chicken cells by inhibiting viral protein expression and viral genome replication.

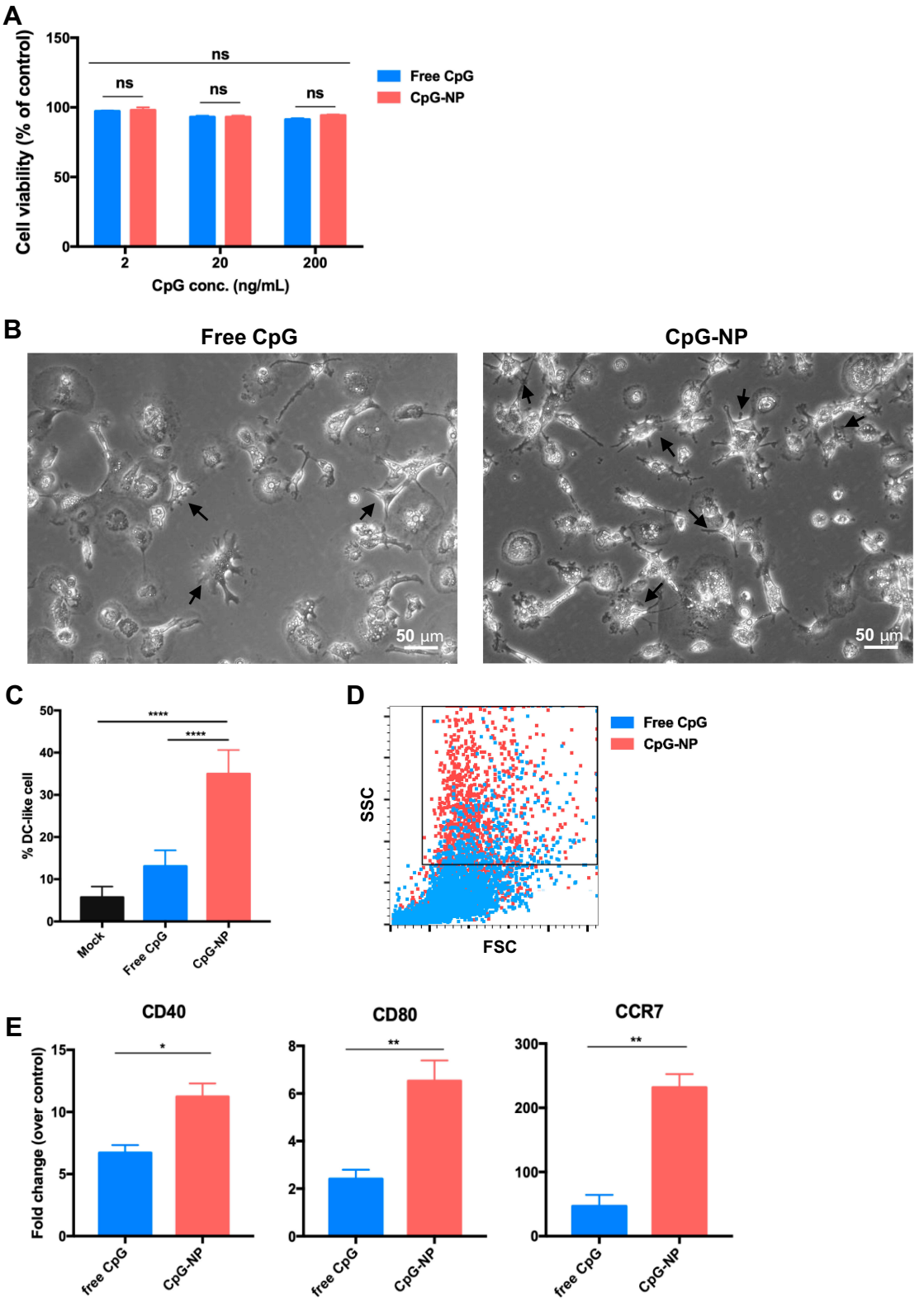

Figure 3 (**A**) chBMDC viability following the treatment with various concentrations of free CpG and CpG-NP. The viability of untreated cell grown in medium for 72 hr was considered to be 100%. Chicken BMDCs were incubated with 200 ng/mL free CpG or CpG-NP for 16 hr. The dendrites of mature chBMDCs were indicated with black arrows (**B**), and the percentage of DCswith dendritic morphology was quantified (**C**). (**D**) Cells were analyzed by flow cytometry, revealing increased side scattering for CpG-NP treated DCs. (**E**) CD40, CD80 and CCR7 mRNA expression levels were measured by qRT-PCR. Error bars represent mean ± SD in (**C**), n=9, other data in the plot present the mean ± SEM, n=3 (ns, nonsignificant; *p ≤ 0.05; **p≤ 0.01, ****p ≤ 0.001).

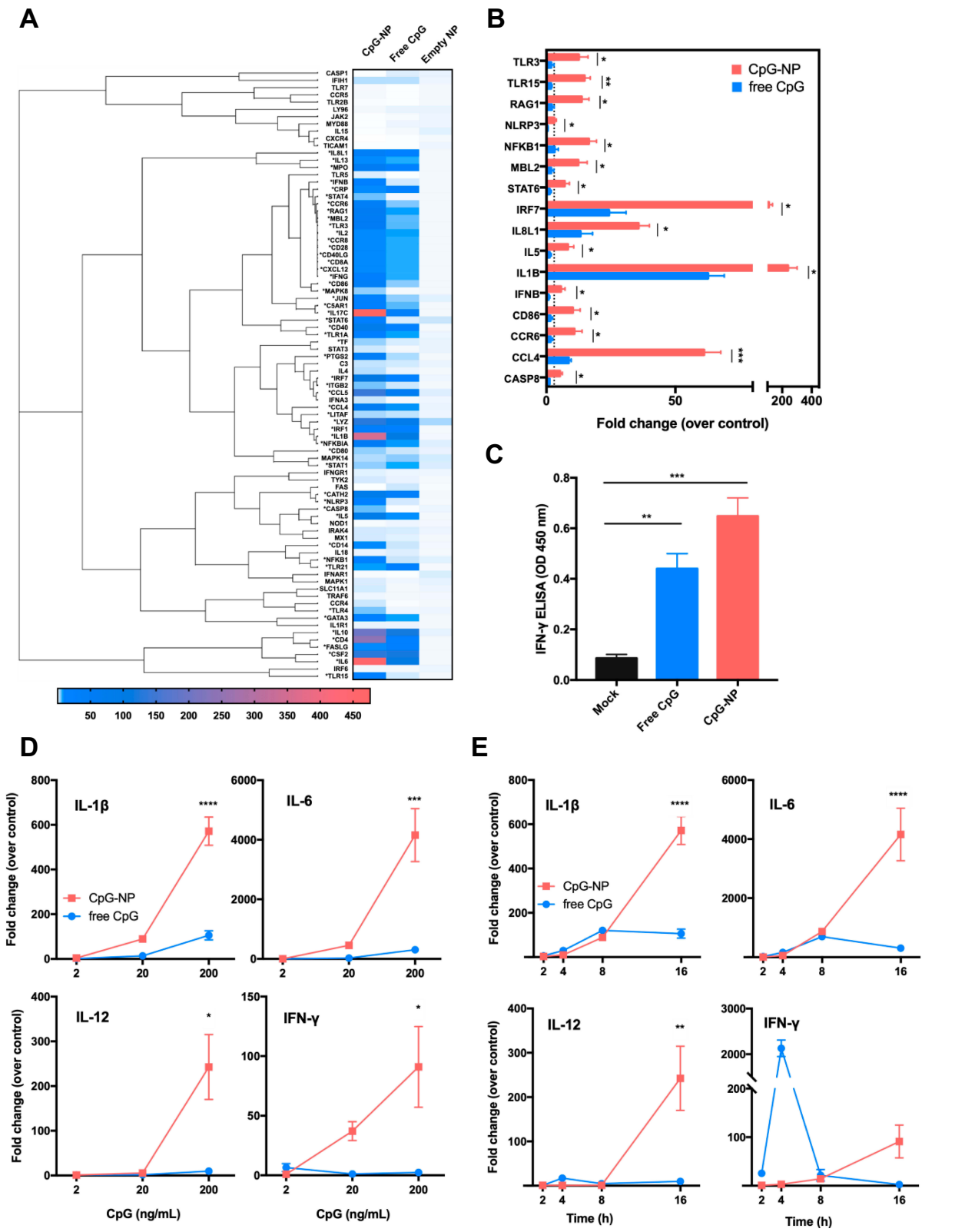

Figure 4 (**A**) Immune gene induction of chBMDCs following the treatment with 200 ng/mL free CpG, CpG-NP or empty NP for 16 hr. Genes labelled with * indicate a more than three-fold stimulation by CpG-NP as compared to free CpG. (**B**) Genes significantly upregulated after the 16-hr treatment of 200 ng/mL CpG-NP as compared to free CpG are shown. (**C**) IFN-γ level in the culture supernatant of chBMDCs was detected by ELISA after 24 hr treatment of CpG-NP, free CpG or mock treatment. (**D**) IL-1β, IL-6, IL-12 and IFN-γ mRNA expression levels of chBMDCs treated with various concentrations of free CpG or CpG-NP for 16 hr were detected by qRT-PCR. (**E**) IL-1β, IL-6, IL-12 and IFN-γ mRNA expression levels of chBMDCs treated with 200 ng/mL of free CpG or CpG-NP were monitored by qRT-PCR at different time points. Data in the plot present the mean ± SEM, n=3 (ns, nonsignificant; *p ≤ 0.05; **p≤ 0.01, ***p ≤ 0.005, ****p ≤ 0.001).

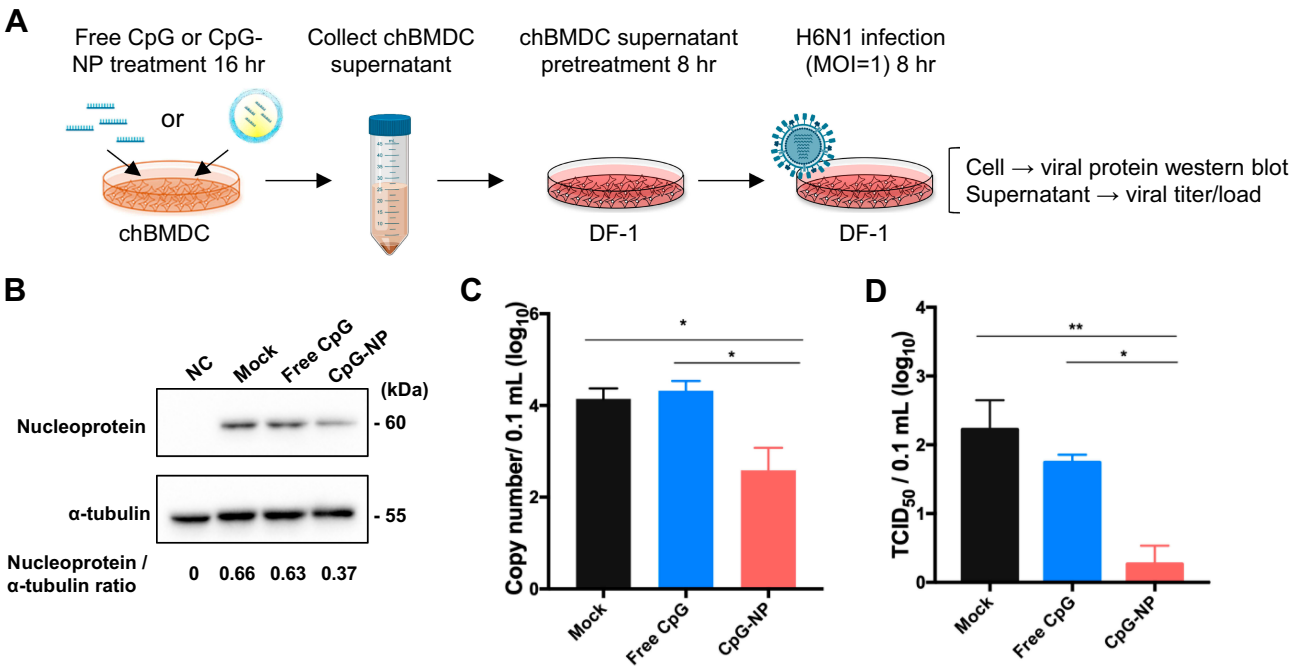

Figure 5 (**A**) Flow chart of DF-1 cell protection test by chBMDC culture supernatant. ChBMDC culture supernatant pretreated DF-1 was infected with MOI 1 H6N1 avian influenza virus for 8 hr. Then, viral nucleoprotein (NP) expression in DF-1 cell was measured by Western blotting and normalized to internal control α-tubulin (**B**). Supernatant from infected DF-1 cell was collected for viral genome quantification (**C**) and $TCID_{50}$ measurement (**D**). Data in the plot present the mean ± SEM, n=3 (*p ≤ 0.05; **p≤ 0.01).

Expression of IBV Spike Receptor Binding Domain (RBD) Protein

According to the previous study, IBV RBD is located at the N-terminus 253 amino acids in the spike protein of IBV M41 strain. Through the pairwise alignment of the spike protein from the M41 and IBV 2296/95 strain, the RBD of 2296/95 strain was putatively located at the N-terminus 19-254 amino acids (Figure 6A). Excluding an 18-aa signal peptide at the very end of N terminal, a 236-aa fragment encoding for rRBD was cloned, fused with two polyhistidine tags (Figure 6A) and expressed in serum free-adapted Sf21 insect cells (Figure S2). As shown in Figure 6B, purified rRBD protein (approximately 55 kDa) was obtained and verified through SDS-PAGE and Western blot using a monoclonal antibody against IBV S1.

Superior Humoral Response and Protection Against Viral Challenge by CpG-NP Adjuvanted Immunization

IBV rRBD protein was used as an antigen for chickens to evaluate the immunostimulatory effect of free CpG or CpG-NP in vivo. The immunization schedule of SPF chickens is shown in Figure 6C. Three groups chickens were subcutaneously immunized at the back between wings with sterile PBS, rRBD protein mixed with free CpG, or rRBD protein mixed with CpG-NP, respectively, and serum was collected after the first booster shot for RBD-specific antibody titration. While anti-rRBD antibody titer of the free CpG adjuvanted rRBD immunization group barely showed differences to that of the PBS control group, chickens receiving CpG-NP adjuvanted rRBD demonstrated nearly 4-fold higher antibody titers in the serum (titer: 5711) and showed a significant difference to the other controls (Figure 6D). After 10^6 EID_{50} of homologous IBV challenge, lung and kidney were collected 7 days post-challenge from each group, and tissues were homogenized for virus re-isolation in SPF embryonic eggs. As shown in Table 2, the CpG-NP adjuvanted immunization resulted a reduced virus replication in both lung and kidney. Overall, the enhanced humoral response and improved protective efficacy provided by CpG-NP adjuvanted protein immunization highlight superior adjuvanticity of nanoparticulate CpG.

Discussion

In this study, we prepared a novel hollow PLGA nanoparticle loaded with CpG ODN 2007 adjuvant, which can be efficiently engulfed by immature chBMDC, potently stimulate chBMDCs' maturation, activate immune response, and promote antiviral activity in vitro and immunostimulatory effects in vivo. While CpG has been widely adopted as an immunostimulatory ligand, this study is the first to

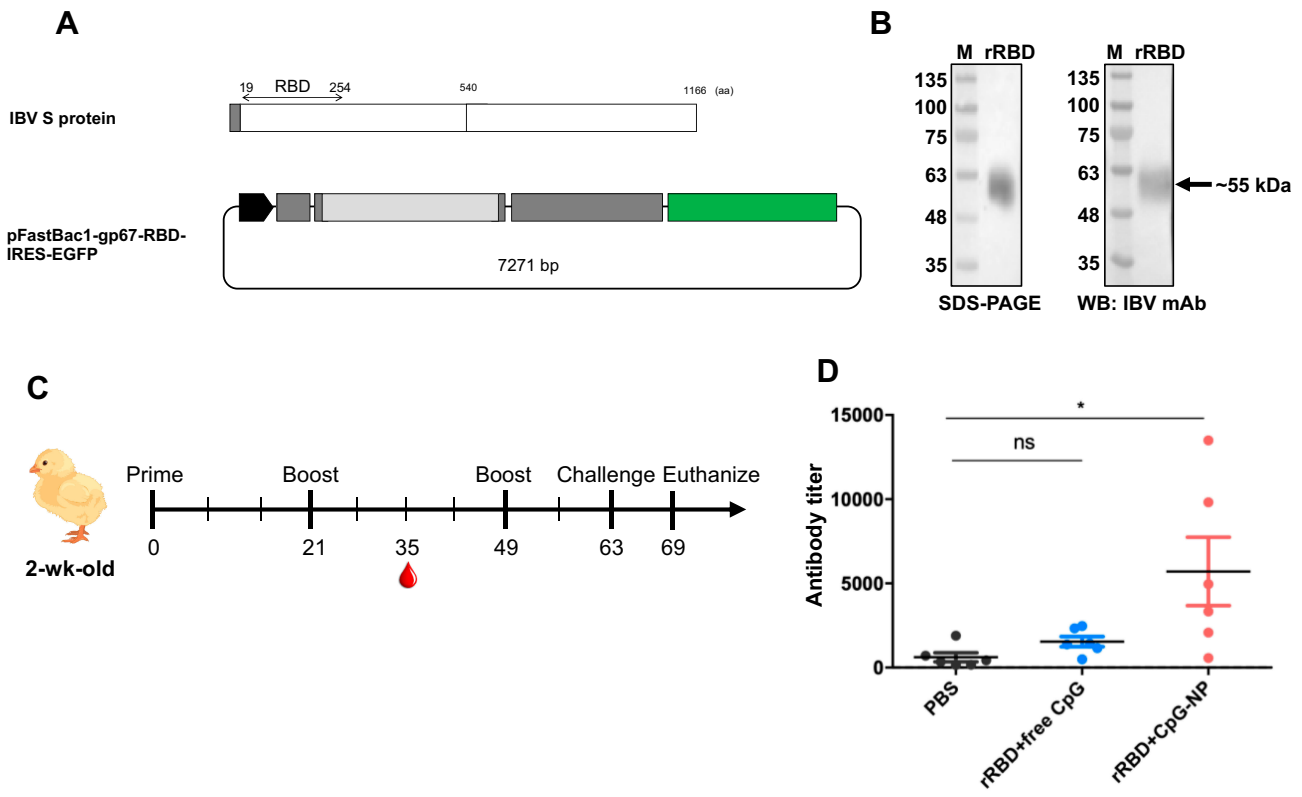

Figure 6 (**A**) Construction and expression of recombinant infectious bronchitis virus receptor-binding domain (rRBD) in insect cell system. (**B**) rRBD expression was checked in stain-free SDS-PAGE and Western blot. (**C**) Experimental design of chicken vaccination of rRBD adjuvanted with free CpG or CpG-NP. (**D**) Specific anti-rRBD antibody in serum was titrated at day 35. Data in the plot present the mean ± SEM, n=6 (ns, nonsignificant, *p ≤ 0.05).

address the previously unelucidated mechanism that contributes to the immune activation in chickens, by using an ex vivo BMDC model. The present nanoformulation scheme yields nanoparticles with a diameter of about 160 nm, which can drain freely in the lymphatic system.[32] We show that the CpG-NP remains stable following storage by freezing or at the room temperature, demonstrating that the nanoparticles can be transported upon freezing and possess adequate stability for practical use. The nanoparticles are stable at the physiological pH, releasing less than 50% of its cargo in 96 hr. At pH 5.0, acid-induced ester hydrolysis facilitates the breakdown of the PLGA nanoparticles and accelerates the CpG release. Thus, the low pH environment in endosome is conducive to CpG release, allowing intracellular TLR21, the CpG receptor in chickens, to be stimulated by the large amount of encapsulated CpG.

Table 2 Virus Re-Isolation Rates from Chickens After Viral Challenge

	PBS	rRBD Plus Free CpG	rRBD Plus CpG-NP
Lung	5/5	4/5	1/5
Kidney	4/5	4/5	2/5

Abbreviations: rRBD, recombinant receptor binding domain; NP, nanoparticle.

Ex vivo culture of chBMDC was used to test the efficacy of encapsulated CpG. Maturation of dendritic cells is essential to its functionalization to process and present internalized antigen, and to express co-stimulator and home to lymph nodes. Morphology and phenotype characterization were used to assess the DC's maturation induced by free CpG or CpG-NP. Both forms of CpG treatment can turn the veiled, round, immature BMDCs to a dendritic morphology, a characteristic of mature DC. Upon dendrite quantification among activated DCs, CpG-NP stimulated DC maturation to a significantly greater extent over free CpG.

Antigen presentation to naïve T cells and initiation of specific adaptive immune responses depend on surface MHC-II-antigen complex as well as co-stimulators of DCs, like CD40, CD80 and CD86. In mammals and chickens, these costimulatory molecules are commonly used as criteria to characterize DCs' maturation.[24,33] After CpG-NP treatment, CD40 and CD80 mRNA expression levels in chBMDC were increased by more than 3-fold as compared to free CpG-treated cells. These two co-stimulators were also detected in the PCR array assay and showed a consistent result. The PCR array also showed a more than 3-fold increase of CD86 following CpG-

NP treatment. In mammals, the CC chemokine receptors 7 (CCR7) plays an important role in controlling the homing of DCs to secondary lymphoid organs where they encounter naïve T cells.[34] Maturation of chicken DCs was confirmed with the upregulation of CCR7.[35] Thus, stimulation of CD40, CD80, CD86 and CCR7 indicated the high potency of CpG-NP to drive chBMDCs to become phenotypically mature.

With the maturation of DCs, secretion of cytokines would mediate the promotion of B cell response to produce antibodies, and to polarize cell-mediated immune responses into either Th1 or Th2 responses. IL-6 is not only a B cell growth factor and plasma cell differentiation inducer,[36] but also plays an essential role in regulating the Th17 and Treg cells, which have functions in protection against bacterial infections and restrain excessive effector T cell responses, respectively.[37] IL-6 mRNA was observed to be expressed in a greater amount under the CpG-NP treatment, which may harbinger a strong B cell maturation response and induction of Th17 response. IL-12 and IL-18 expression trigger Th1 cell differentiation, promoting cell-mediated immune responses,[38] and they are required for IFN-γ production.[39,40] On the other hand, IL-10 regulates T cells polarization to Th2 and inhibits IFN-γ production in DCs.[41] Although both IL-10 and IL-12 were upregulated by CpG-NP treatment, the sustained expression of IL-12 and IL-18 supported the continuous production of IFN-γ. In contrast, free CpG-treated cells expressed low levels of IL-12 may account for the transient expression of IFN-γ. Another Th cell polarization regulator, IL-4, was minimally stimulated by either the nanoformulation or the free form of CpG. Taken together, encapsulated CpG-NP is more effective at polarizing CD4+ T cell into Th1 rather than Th2 phenotype. Another cytokine, CD40 ligand (CD40LG), which is known as a B cell regulator responsible for cell differentiation in the chicken harderian gland,[42,43] was also upregulated from CpG-NP treated cells. In addition, IL-1β was one of the most significantly upregulated genes in the panel. Previously, IL-1β was shown to induce other cytokines' expression and enhance mucosal IgA in mice and chickens when co-administered intranasally with OVA or attenuated Newcastle disease virus.[44] Considering the stimulation of CD40LG and IL-1β, the potential of CpG-NP to act as mucosal targeting adjuvant and promote IgA secretion presents an appealing aspect for future studies.

With the significant expression of cytokines and TLR signaling genes in CpG-NP treated cells, it is expected that CpG-NP can prime the activation of virus resistant state and improve immune responses through DC priming. IFN-β, a critical marker of innate immune activation that constitutes host defense and activates adaptive immune responses, was upregulated by CpG-NP but not by free CpG in this study. Pretreatment with supernatant derived from CpG-NP-primed chBMDC was sufficient to trigger DF-1 cells' antiviral state and protection against subsequent H6N1 infection, indicating the activation of rapid, non-specific innate immune response. In addition, CpG-NP was shown to be capable of activating the adaptive immunity in vivo as evidenced by elevated antigen-specific antibody responses. More importantly, the antibody titer observed from the CpG-NP adjuvanted group was comparable level to that following live IBV infection.[45] This robust humoral response presumably led to improved protection in chickens after challenge. The CpG-NP presents a promising candidate for antiviral and vaccine applications in chickens and other poultry animals.

Conclusions

A PLGA hollow nanoparticle loaded with CpG ODN 2007 adjuvant showed evidence of improved innate immune stimulating effectiveness and long-lasting immunostimulatory ability ex vivo and in vivo in chickens, as compared to free CpG. This enhanced immune stimulation benefits from the high stability and controlled release of internal component of nanoparticles that improve cellular delivery, lymphoid organ targeting, and sustainable DC activation. The enhanced DC activation is found to activate a plethora of cytokine expression that contribute to the induction of antiviral state. In addition, utility of the CpG-NP as a vaccine adjuvant is shown to significantly elevate humoral immune responses and antiviral protectivity.

Acknowledgments

This work was supported by the Ministry of Science and Technology of Taiwan (106-2311-B-002-030-MY3, 107-2321-B-002-024, 108-2321-B-002-015, 109-2321-B-002-033). Technical assistance provided by the Technology Commons in College of Life Science and the Joint Center for Instruments and Researches in College of Bioresources and Agriculture of National Taiwan University is appreciated.

Disclosure

The authors report no conflicts of interest in this work.

References

1. Ninomiya A, Imai M, Tashiro M, Odagiri T. Inactivated influenza H5N1 whole-virus vaccine with aluminum adjuvant induces homologous and heterologous protective immunities against lethal challenge with highly pathogenic H5N1 avian influenza viruses in a mouse model. *Vaccine*. 2007;25(18):3554–3560. doi:10.1016/j.vaccine.2007.01.083
2. Gupta RK. Aluminum compounds as vaccine adjuvants. *Adv Drug Deliv Rev*. 1998;32(3):155–172. doi:10.1016/S0169-409X(98)00008-8

3. Chu RS, Targoni OS, Krieg AM, Lehmann PV, Harding CV. CpG oligodeoxynucleotides act as adjuvants that switch on T helper 1 (Th1) immunity. *J Exp Med*. 1997;186(10):1623–1631. doi:10.1084/jem.186.10.1623
4. Klinman DM, Currie D, Gursel I, Verthelyi D. Use of CpG oligodeoxynucleotides as immune adjuvants. *Immunol Rev*. 2004;199 (1):201–216. doi:10.1111/j.0105-2896.2004.00148.x
5. Akira S, Takeda K. Toll-like receptor signalling. *Nat Rev Immunol*. 2004;4(7):499. doi:10.1038/nri1391
6. Brownlie R, Zhu J, Allan B, et al. Chicken TLR21 acts as a functional homologue to mammalian TLR9 in the recognition of CpG oligodeoxynucleotides. *Mol Immunol*. 2009;46(15):3163–3170. doi:10.1016/j.molimm.2009.06.002
7. Taghavi A, Allan B, Mutwiri G, et al. Enhancement of immunoprotective effect of CpG-ODN by formulation with polyphosphazenes against E. coli septicemia in neonatal chickens. *Curr Drug Deliv*. 2009;6(1):76–82. doi:10.2174/156720109787048221
8. Taghavi A, Allan B, Mutwiri G, et al. Protection of neonatal broiler chicks against salmonella typhimurium septicemia by DNA containing CpG motifs. *Avian Dis*. 2008;52(3):398–406. doi:10.1637/8196-121907-Reg
9. St. Paul M, Barjesteh N, Brisbin JT, et al. Effects of ligands for toll-like receptors 3, 4, and 21 as adjuvants on the immunogenicity of an avian influenza vaccine in chickens. *Viral Immunol*. 2014;27 (4):167–173. doi:10.1089/vim.2013.0124
10. Dar A, Potter A, Tikoo S, et al. CpG oligodeoxynucleotides activate innate immune response that suppresses infectious bronchitis virus replication in chicken embryos. *Avian Dis*. 2009;53(2):261–267. doi:10.1637/8560-121808-Reg.1
11. Zhang L, Zhang M, Li J, Cao T, Tian X, Zhou F. Enhancement of mucosal immune responses by intranasal co-delivery of newcastle disease vaccine plus CpG oligonucleotide in SPF chickens in vivo. *Res Vet Sci*. 2008;85(3):495–502. doi:10.1016/j.rvsc.2008.02.006
12. Krieg AM. CpG motifs in bacterial DNA and their immune effects. *Annu Rev Immunol*. 2002;20(1):709–760. doi:10.1146/annurev.immunol.20.100301.064842
13. Roda JM, Parihar R, Carson WE. CpG-containing oligodeoxynucleotides act through TLR9 to enhance the NK cell cytokine response to antibody-coated tumor cells. *J Immunol*. 2005;175(3):1619–1627. doi:10.4049/jimmunol.175.3.1619
14. Paul MS, Mallick AI, Read LR, et al. Prophylactic treatment with toll-like receptor ligands enhances host immunity to avian influenza virus in chickens. *Vaccine*. 2012;30(30):4524–4531. doi:10.1016/j.vaccine.2012.04.033
15. Hafner AM, Corthesy B, Merkle HP. Particulate formulations for the delivery of poly (I: C) as vaccine adjuvant. *Adv Drug Deliv Rev*. 2013;65(10):1386–1399. doi:10.1016/j.addr.2013.05.013
16. Kumar S, Kesharwani SS, Kuppast B, Bakkari MA, Tummala H. Pathogen-mimicking vaccine delivery system designed with a bioactive polymer (inulin acetate) for robust humoral and cellular immune responses. *J Control Release*. 2017;261:263–274. doi:10.1016/j.jconrel.2017.06.026
17. Rajput MK, Kesharwani SS, Kumar S, Muley P, Narisetty S, Tummala H. Dendritic cell-targeted nanovaccine delivery system prepared with an immune-active polymer. *ACS Appl Mater Interfaces*. 2018;10(33):27589–27602. doi:10.1021/acsami.8b02019
18. Lin LCW, Huang CY, Yao BY, et al. Viromimetic STING agonist-loaded hollow polymeric nanoparticles for safe and effective vaccination against Middle East respiratory syndrome coronavirus. *Adv Funct Mater*. 2019;29(28):1807616. doi:10.1002/adfm.201807616
19. Chattopadhyay S, Chen JY, Chen HW, Hu CJ. Nanoparticle vaccines adopting virus-like features for enhanced immune potentiation. *Nanotheranostics*. 2017;1(3):244–260. doi:10.7150/ntno.19796
20. Singh SM, Alkie TN, Nagy É, Kulkarni RR, Hodgins DC, Sharif S. Delivery of an inactivated avian influenza virus vaccine adjuvanted with poly (D, L-lactic-co-glycolic acid) encapsulated CpG ODN induces protective immune responses in chickens. *Vaccine*. 2016;34 (40):4807–4813. doi:10.1016/j.vaccine.2016.08.009
21. Chen H-W, Cheng JX, Liu M-T, et al. Inhibitory and combinatorial effect of diphyllin, a v-ATPase blocker, on influenza viruses. *Antiviral Res*. 2013;99(3):371–382. doi:10.1016/j.antiviral.2013.06.014
22. Li YT, Chen TC, Lin SY, et al. Emerging lethal infectious bronchitis coronavirus variants with multiorgan tropism. *Transbound Emerg Dis*. 2019.
23. Tsai C-T, Tsai H-F, Wang C-H. Detection of infectious bronchitis virus strains similar to Japan in Taiwan. *J Vet Med Sci*. 2016;15–0609.
24. Wu Z, Rothwell L, Young JR, Kaufman J, Butter C, Kaiser P. Generation and characterization of chicken bone marrow-derived dendritic cells. *Immunology*. 2010;129(1):133–145. doi:10.1111/j.1365-2567.2009.03129.x
25. Hu C-MJ, Chen Y-T, Fang Z-S, Chang W-S, Chen H-W. Antiviral efficacy of nanoparticulate vacuolar ATPase inhibitors against influenza virus infection. *Int J Nanomedicine*. 2018;13:8579. doi:10.2147/IJN.S185806
26. Chen HW, Fang ZS, Chen YT, et al. Targeting and enrichment of viral pathogen by cell membrane cloaked magnetic nanoparticles for enhanced detection. *ACS Appl Mater Interfaces*. 2017;9 (46):39953–39961. doi:10.1021/acsami.7b09931
27. Promkuntod N, Van Eijndhoven R, De Vrieze G, Gröne A, Verheije M. Mapping of the receptor-binding domain and amino acids critical for attachment in the spike protein of avian coronavirus infectious bronchitis virus. *Virology*. 2014;448:26–32. doi:10.1016/j.virol.2013.09.018
28. Hsieh M-S, He J-L, Wu T-Y, Juang R-H. A secretary bi-cistronic baculovirus expression system with improved production of the HA1 protein of H6 influenza virus in insect cells and spodoptera litura larvae. *J Immunol Methods*. 2018;459:81–89. doi:10.1016/j.jim.2018.06.001
29. Liu I-L, Lin Y-C, Lin Y-C, Jian C-Z, Cheng I-C, Chen H-W. A novel immunochromatographic strip for antigen detection of avian infectious bronchitis virus. *Int J Mol Sci*. 2019;20(9):2216. doi:10.3390/ijms20092216
30. Van Goor A, Slawinska A, Schmidt CJ, Lamont SJ. Distinct functional responses to stressors of bone marrow derived dendritic cells from diverse inbred chicken lines. *Dev Comp Immunol*. 2016;63:96–110. doi:10.1016/j.dci.2016.05.016
31. Grassi F, Dezutter-Dambuyant C, McIlroy D, et al. Monocyte-derived dendritic cells have a phenotype comparable to that of dermal dendritic cells and display ultrastructural granules distinct from birbeck granules. *J Leukoc Biol*. 1998;64(4):484–493. doi:10.1002/jlb.64.4.484
32. Manolova V, Flace A, Bauer M, Schwarz K, Saudan P, Bachmann MF. Nanoparticles target distinct dendritic cell populations according to their size. *Eur J Immunol*. 2008;38(5):1404–1413. doi:10.1002/eji.200737984
33. Steinman RM. The dendritic cell system and its role in immunogenicity. *Annu Rev Immunol*. 1991;9(1):271–296. doi:10.1146/annurev.iy.09.040191.001415
34. Sallusto F, Schaerli P, Loetscher P, et al. Rapid and coordinated switch in chemokine receptor expression during dendritic cell maturation. *Eur J Immunol*. 1998;28(9):2760–2769. doi:10.1002/(SICI)1521-4141(199809)28:09<2760::AID-IMMU2760>3.0.CO;2-N
35. Wu Z, Hu T, Kaiser P. Chicken CCR6 and CCR7 are markers for immature and mature dendritic cells respectively. *Dev Comp Immunol*. 2011;35(5):563–567. doi:10.1016/j.dci.2010.12.015
36. Dienz O, Eaton SM, Bond JP, et al. The induction of antibody production by IL-6 is indirectly mediated by IL-21 produced by CD4+ T cells. *J Exp Med*. 2009;206(1):69–78. doi:10.1084/jem.20081571
37. Kimura A, Kishimoto T. IL-6: regulator of Treg/Th17 balance. *Eur J Immunol*. 2010;40(7):1830–1835. doi:10.1002/eji.201040391
38. Manetti R, Parronchi P, Giudizi MG, et al. Natural killer cell stimulatory factor (interleukin 12 [IL-12]) induces T helper type 1 (Th1)-specific immune responses and inhibits the development of IL-4-producing Th cells. *J Exp Med*. 1993;177(4):1199–1204. doi:10.1084/jem.177.4.1199

39. Seder RA, Gazzinelli R, Sher A, Paul WE. Interleukin 12 acts directly on CD4+ T cells to enhance priming for interferon gamma production and diminishes interleukin 4 inhibition of such priming. *Proc Natl Acad Sci*. 1993;90(21):10188–10192. doi:10.1073/pnas.90.21.10188
40. Stoll S, Jonuleit H, Schmitt E, et al. Production of functional IL-18 by different subtypes of murine and human dendritic cells (DC): DC-derived IL-18 enhances IL-12-dependent Th1 development. *Eur J Immunol*. 1998;28(10):3231–3239. doi:10.1002/(SICI)1521-4141-(199810)28:10<3231::AID-IMMU3231>3.0.CO;2-Q
41. De Smedt T, Van Mechelen M, De Becker G, Urbain J, Leo O, Moser M. Effect of interleukin-10 on dendritic cell maturation and function. *Eur J Immunol*. 1997;27(5):1229–1235. doi:10.1002/eji.1830270526
42. Tregaskes CA, Glansbeek HL, Gill AC, Hunt LG, Burnside J, Young JR. Conservation of biological properties of the CD40 ligand, CD154 in a non-mammalian vertebrate. *Dev Comp Immunol*. 2005;29(4):361–374. doi:10.1016/j.dci.2004.09.001
43. Kothlow S, Kaspers B. The avian respiratory immune system. *Avian Immunol*. 2008;1:273–288.
44. Staats HF, Ennis FA. IL-1 is an effective adjuvant for mucosal and systemic immune responses when coadministered with protein immunogens. *J Immunol*. 1999;162(10):6141–6147.
45. Lin S-Y, Li Y-T, Chen Y-T, Chen T-C, Hu C-MJ, Chen H-W. Identification of an infectious bronchitis coronavirus strain exhibiting a classical genotype but altered antigenicity, pathogenicity, and innate immunity profile. *Sci Rep*. 2016;6(1):37725. doi:10.1038/srep37725
46. Wang BK, Mao YL, Gong L, et al. Glycyrrhizic acid activates chicken macrophages and enhances their salmonella-killing capacity in vitro. *J Zhejiang Univ Sci B*. 2018;19(10):785–795. doi:10.1631/jzus.B1700506
47. Jiang H, Yang H, Kapczynski DR. Chicken interferon alpha pretreatment reduces virus replication of pandemic H1N1 and H5N9 avian influenza viruses in lung cell cultures from different avian species. *Virol J*. 2011;8(1):447. doi:10.1186/1743-422X-8-447
48. Liu H, Zhang M, Han H, Yuan J, Li Z. Comparison of the expression of cytokine genes in the bursal tissues of the chickens following challenge with infectious bursal disease viruses of varying virulence. *Virol J*. 2010;7(1):364. doi:10.1186/1743-422X-7-364

International Journal of Nanomedicine Dovepress

Publish your work in this journal

The International Journal of Nanomedicine is an international, peer-reviewed journal focusing on the application of nanotechnology in diagnostics, therapeutics, and drug delivery systems throughout the biomedical field. This journal is indexed on PubMed Central, MedLine, CAS, SciSearch®, Current Contents®/Clinical Medicine, Journal Citation Reports/Science Edition, EMBase, Scopus and the Elsevier Bibliographic databases. The manuscript management system is completely online and includes a very quick and fair peer-review system, which is all easy to use. Visit http://www.dovepress.com/testimonials.php to read real quotes from published authors.

Submit your manuscript here: https://www.dovepress.com/international-journal-of-nanomedicine-journal